

# TECHNIQUES FOR OPTICAL OBSERVATIONS OF SPACE DEBRIS — PERFORMANCE TESTS WITH THE NEW 1 METER ZIMMERWALD TELESCOPE

T. Schildknecht, U. Hugentobler, G. Beutler

Astronomical Institute, University of Berne, Switzerland

## ABSTRACT

The use of CCD detectors opened new prospects for optical observations of space debris. Especially for surveys in the geostationary ring (GEO) and in the geostationary transfer orbit (GTO) region optical techniques outperform the RADAR observations in terms of the minimum detectable object size. The essential characteristics of the CCD observation techniques developed at the Astronomical Institute of the University of Berne (AIUB) are presented. These include optimized observation scenarios and automated CCD data processing. A limited survey in the geostationary ring was carried out using the new 1 m Zimmerwald Laser and Astrometry Telescope (ZIM-LAT). All controlled and catalogued objects in GEO were successfully observed. In addition 25 objects with inclinations exceeding  $0.5^\circ$  were found. Most of them are probably catalogued.

## 1. INTRODUCTION

The use of CCD detectors opened new prospects for optical observations of space debris. The full potential of modern optical observations may be exploited best for high altitude orbits. For surveys in the geostationary ring (GEO) and in the geostationary transfer orbit (GTO) region optical techniques are particularly well suited and outperform the RADAR observations in terms of minimum detectable object size. We will therefore focus on these most promising orbits, although optical techniques may also be applied to low Earth orbiters (LEOs).

Optical observations of the GEO and the GTO regions have been carried out for decades by the national surveillance networks of the United States, Russia and other space faring nations. However, these observations were limited in two respects: a) in most cases operational requirements did not allow these networks to perform extended searches for uncatalogued objects (also called uncorrelated targets (UCTs)), and b) apart from a few experimental stations these networks are equipped with vidicon type sensors which have a reduced sensitivity compared to CCDs.

It is known that for the GEO/GTO region the existing catalogues of tracked objects (the US Space Command and the Russian catalogue) are not complete even when considering only the 'known' objects. There are e.g. apogee boost motors (ABMs), mission related objects like large covers of sizes up to  $1 \text{ m}^2$ , and even entire satellites (e.g. TV Sat-1) which were either never tracked or lost after their end of live. Furthermore, there were at least two breakups observed in GEO (Titan upper stage in 1992, and an Ekran satellite in 1972) and many more in the GTO. It is thus obvious that an unknown population of small debris must exist in GEO and GTO.

## 2. THE ZIMMERWALD 1 METER TELESCOPE

The Zimmerwald 1 m telescope is contained in one dome of the observatory of the AIUB located about 8 km south of Berne at an altitude of 950 m above sea level. It was designed as a multi-purpose instrument with two main applications: a) satellite laser ranging (SLR), planned to be mainly a daytime operation in near future, and b) astrometry of moving objects (e.g. satellites, space debris). The different requirements resulted in a very compact instrument on an alt-azimuth mount (allowing slew rates of up to  $30^\circ$  per second) with five focal stations: a Coudé focus and four focal reducers (F/1.2, two F/4, F/8) on a large derotator platform at the Nasmyth focus (see Figure 1). The maximum field of view is  $40'$  (at the F/1.2 and at the F/4).

For survey applications we mainly use the F/1.2 focus and a small  $512 \times 512$  front side illuminated CCD. Given the pixel size of  $20 \mu\text{m}$  this results in a field of view of  $27' \times 27'$  and an image scale of approximately  $3.2$  per pixel. Precise astrometric measurements are performed with the F/4 focus with an image scale of about  $1''$  per pixel. In the near future a  $2k \times 2k$  CCD ( $13.5 \mu\text{m}$  pixel size) will be operational at the F/4 focus ( $0.7''$  per pixel,  $24' \times 24'$  field of view). This CCD will have two readout channels with a high readout rate ( $160 \text{ kpixel/sec/channel}$ ). Due to the much better optical quality of the F/4 focus with respect to the F/1.2 focus this CCD chip will be our preferred sensor for survey applications.



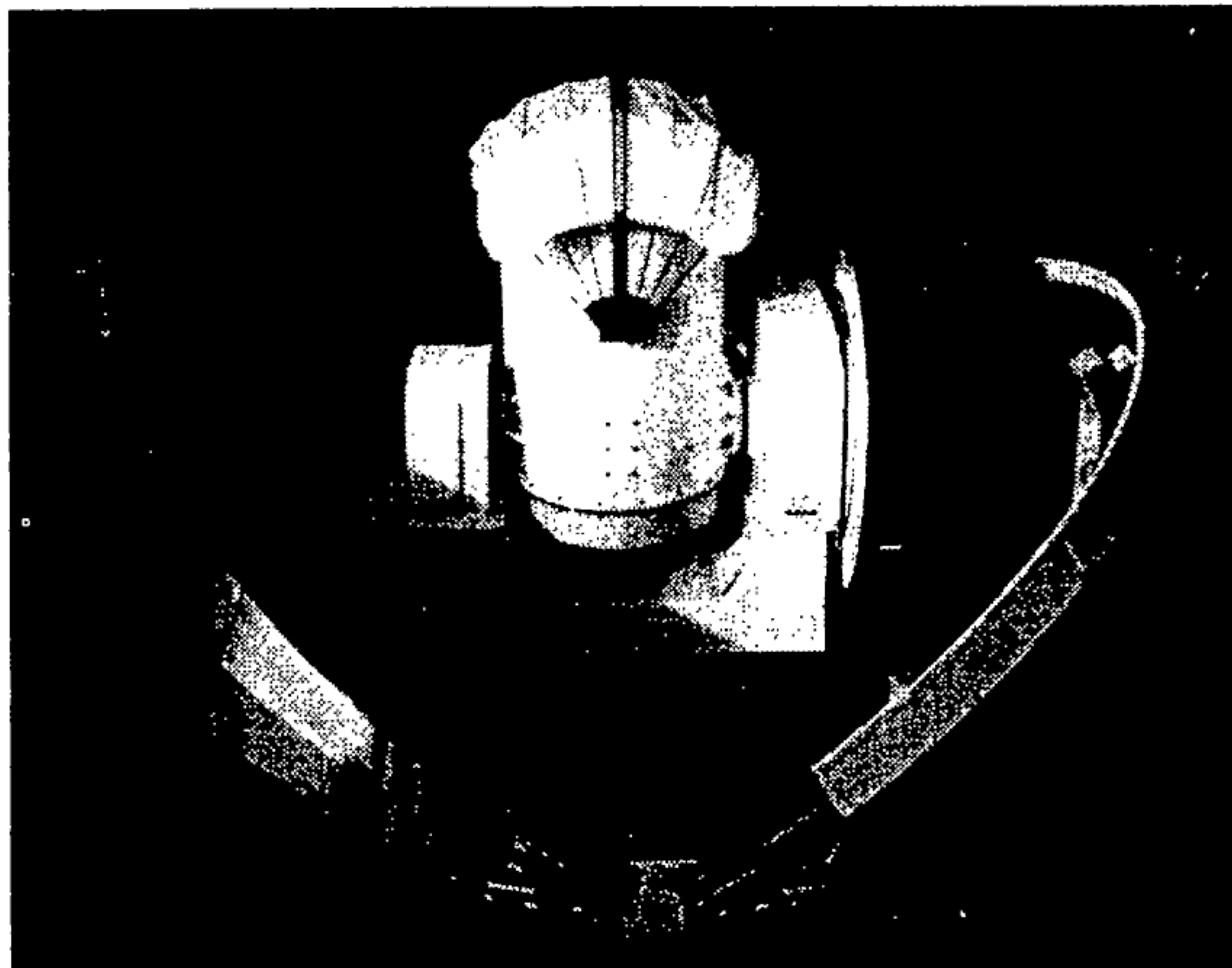


Figure 1. The new Zimmerwald 1 m telescope with its protecting sun cover closed. To the right the partly uncovered derotator platform holding the cameras is visible.

### 3. DETECTION TECHNIQUES / DETECTION LIMITS

#### 3.1. Observation Scenarios, Processing Techniques

The large amount of images produced during a survey clearly asks for automated image processing and object search. The main task consists of the discrimination of moving objects with respect to the stellar background. In astronomy there is a variety of sophisticated object identification algorithms, e.g., to discern stars from galaxies. In the case of debris surveys the required processing time (i.e. 8 MB of data for a 2k x 2k CCD) prevents the use of such algorithms, however. The processing of a single frame should be performed in about the same time as required for the exposure. Otherwise the data may not be treated in near real time or its processing would need more time than the observations (which is unacceptable for a 'continuous' survey). The short exposure times of a few seconds require specialized processing algorithms.

A rapid processing technique has been developed for GEO/GTO objects to compare search frames with a reference frame of the same field in the sky. This comparison is not done directly, e.g., by subtracting the reference frame from the search frame, but by masking the search frame with a template consisting of the objects found on the reference frame. The remaining part of the search frame is then scanned for any objects (which by definition were not on the reference frame). Compared to the subtraction method this technique has several advantages. It does in particular not depend on subtle details of the individual exposures (e.g., slightly different exposure

times generating residuals for all objects in the difference frame). In any case the noise in the reference should be reduced by using the average of several frames. This averaging procedure is equivalent to using a long exposure time in the sidereostatic case (for details see Ref. 1).

In order to re-use the mentioned masks as long as possible it is necessary to adapt the observation scenarios in the sense that the same field in the sky is scanned several times. A 'star-fixed' field will in fact sweep through the GEO region with an angular velocity of 15' per minute (i.e., scanning a stripe with given declination). Depending on the actual exposure and CCD readout time, continuous observations of the same sky field will yield frames with different overlapping factor with respect to an Earth fixed system. The procedure may be optimized by scanning several stripes in parallel.

The detection probability for debris objects may be maximized by a) observing in regions of highest apparent density for a given orbit type, b) by optimizing the S/N on each exposure, and c) by observing the objects when they are brightest.

The first requirement is met by observing the objects at the regions of slowest apparent motion which are the culmination regions for GEO orbits and the apogee regions for GTO respectively.

Optimization of the S/N may be achieved by tracking with the expected motion of the objects during the exposures. For perfectly geostationary objects the telescope should simply be fixed ('drives off') during the exposure. In any case the exposure time must be limited to either a few ten pixel crossing times of the background stars or a few pixel crossing times of the objects of interest in the case of siderostatic tracking (Ref. 1). All frames of the test search campaign were exposed for 5 seconds with the telescope fixed during the exposure. This resulted in elongated images of the background stars of about 23 pixels in length.

The third requirement implies that we must observe the objects at small phase angles (best solar illumination). We must, however, avoid the shadow cone of the Earth! Objects are therefore brightest at the limb of the shadow cone which means just before or after eclipse.

#### 3.2. Detection Limits

The actual detection limit of the entire observation system depends on the quality of the observation site, the efficiency of the detector and telescope hardware combination, as well as the ability of the pro-



cessing algorithms to detect faint sources within the sky background noise.

The quality of the observation defines the S/N 'at the entrance of the telescope'. A poor seeing (caused by atmospheric turbulence) will spread the signal of a point source over a larger solid angle (the so-called seeing disk) and hence reduces the S/N due to the noise contribution of the sky background. The atmospheric transparency and the sky background brightness are additional factors directly limiting the S/N.

In the same sense the telescope/sensor combination may degrade the S/N, e.g., by spreading the light of a point source over a large area in the focal plane (due to poor optics) and by the contribution of the detector readout noise. For CCD detectors the pixel size and the focal length should be matched: Ideally the image of a point source should extend over a few pixels. If the pixels are too small (or the focal length too big) the light is dispersed over many pixels, each one contributing a fixed amount of noise during the readout process. If, on the other hand, the pixels are large compared to the size of the seeing disk (i.e., the entire seeing disk is contained in one pixel), pixels containing object images will also contain an unnecessarily large contribution from the sky background.

Figure 2 gives the limiting magnitude as a function of exposure time for different S/N for the F/1.2 focal station of the Zimmerwald 1 m telescope. The calculations are based on the measured sky brightness of  $19m_v$  per arcsecond square, the known properties

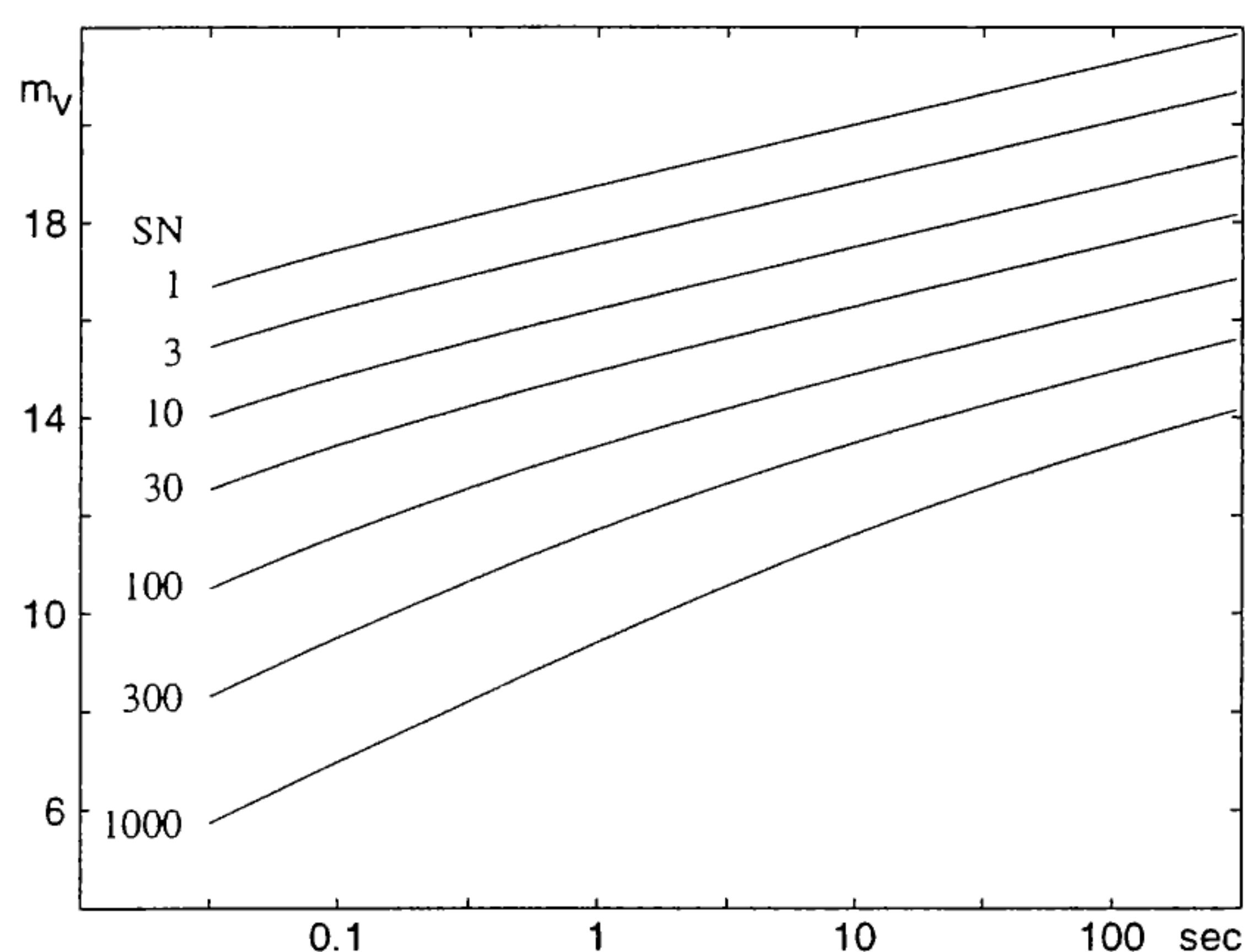


Figure 2. Limiting magnitude as a function of exposure time for different S/N. The calculations are for the F/1.2 focal station of the Zimmerwald 1 m telescope and a sky background of  $19m_v$  per square arcsecond. The automated algorithms detect objects down to a S/N of about 5 to 10.

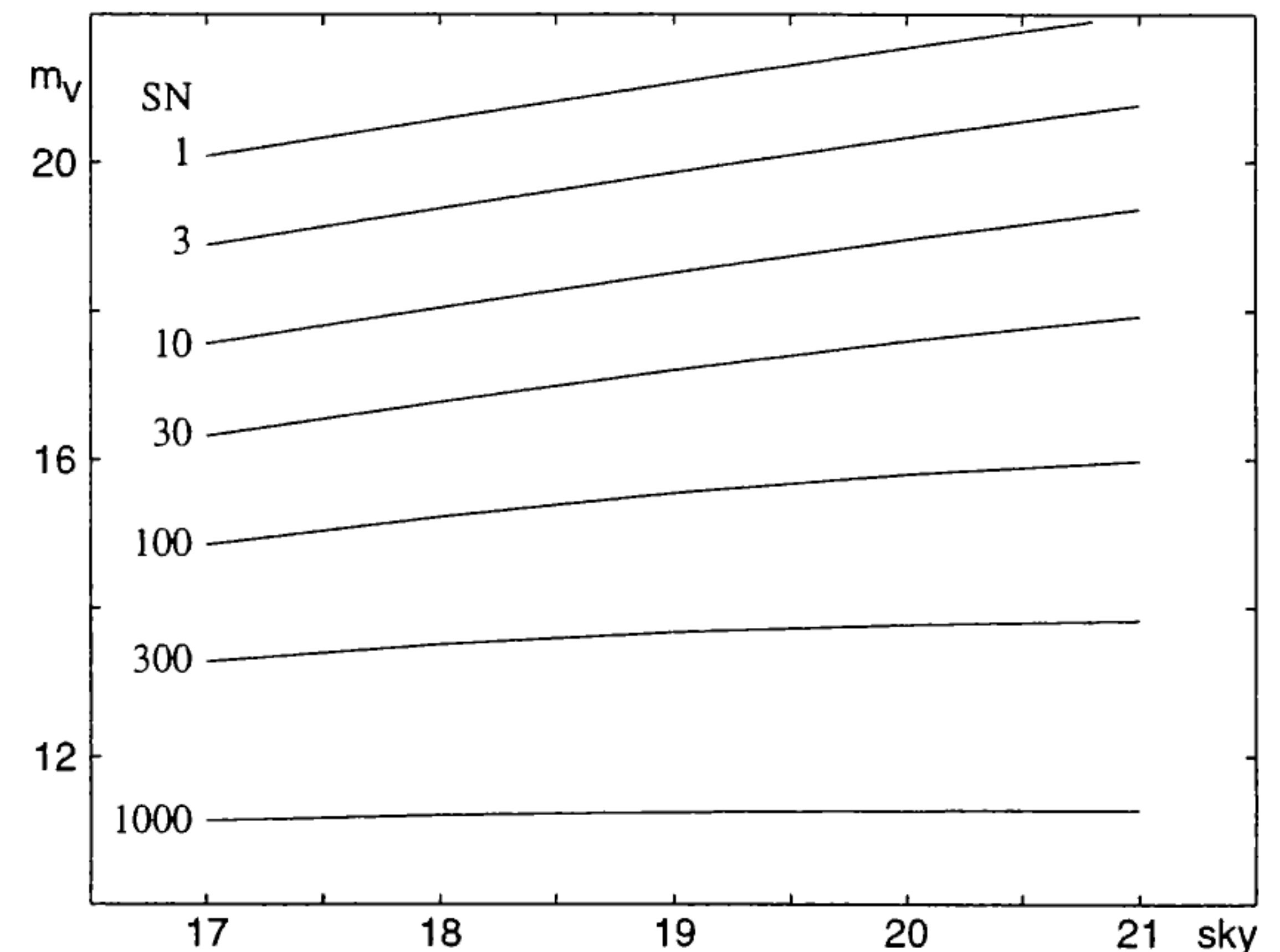


Figure 3. Limiting magnitude as a function of sky background (in arcsecond square) for different S/N. The calculations are for the F/4 focal station of the Zimmerwald 1 m telescope, and an exposure time of 5 seconds. The automated algorithms detect objects down to a S/N of about 5 to 10.

of the CCD detector (readout noise, quantum efficiency) and of the telescope (transmittance), as well as on the site conditions (seeing and atmospheric extinction). The automated algorithms safely detect objects down to a S/N of about 5 to 10. The resulting detection limit of about  $17m_v$  for a 5 second exposure is very moderate for a 1 m telescope. It is entirely due to the high sky background and the large CCD pixel size of  $3''.2$ . The limiting magnitude for the F/4 focal station with respect to the sky background and for different S/N is given in Figure 3. In this case an exposure time of 5 seconds was used.

#### 4. GEO POPULATION CHARACTERISTICS

##### 4.1. Density of Catalogued Objects

Currently more than 600 objects are catalogued in and near the geostationary region. About 465 of them are spacecraft, the rest are rocket upper stages, apogee boost motors, and fragments (Ref. 2). Only about 130 satellites are controlled, about 150 were put into super-geostationary orbits. All remaining objects are drifting or librating near the geostationary ring.

The smallest catalogued objects are about one meter in diameter. The visual magnitude of such objects is (for optimum phase angle) around  $16m_v$  assuming a typical albedo of 0.08 (Ref. 3).

The orbits of the catalogued geostationary objects show a systematic distribution due to the gravitational perturbations from Sun, Moon, and the ob-



lateness of the Earth. These perturbations induce a precession of the orbital planes of the uncontrolled objects around a stable plane which is inclined by  $7.5^\circ$  with respect to the equatorial plane (Ref. 4). The precession period is about 53 years. The orbits of the first satellites put into orbit in the second half of the sixties therefore already reached the maximum inclination of  $15^\circ$ .

The mean apparent density of the catalogued objects on the celestial sphere is given in Figure 4 based on the inclinations and the right ascensions of the ascending nodes given in Ref. 5. The systematic distribution of the satellite orbits due to the orbit precession is clearly visible. The perturbations cause the ascending nodes to drift backwards in right ascension with increasing inclination. The result of this behaviour is an increased object density — a kind of a caustic — at negative declinations close to the ascending nodes and at positive declinations close to the descending nodes.

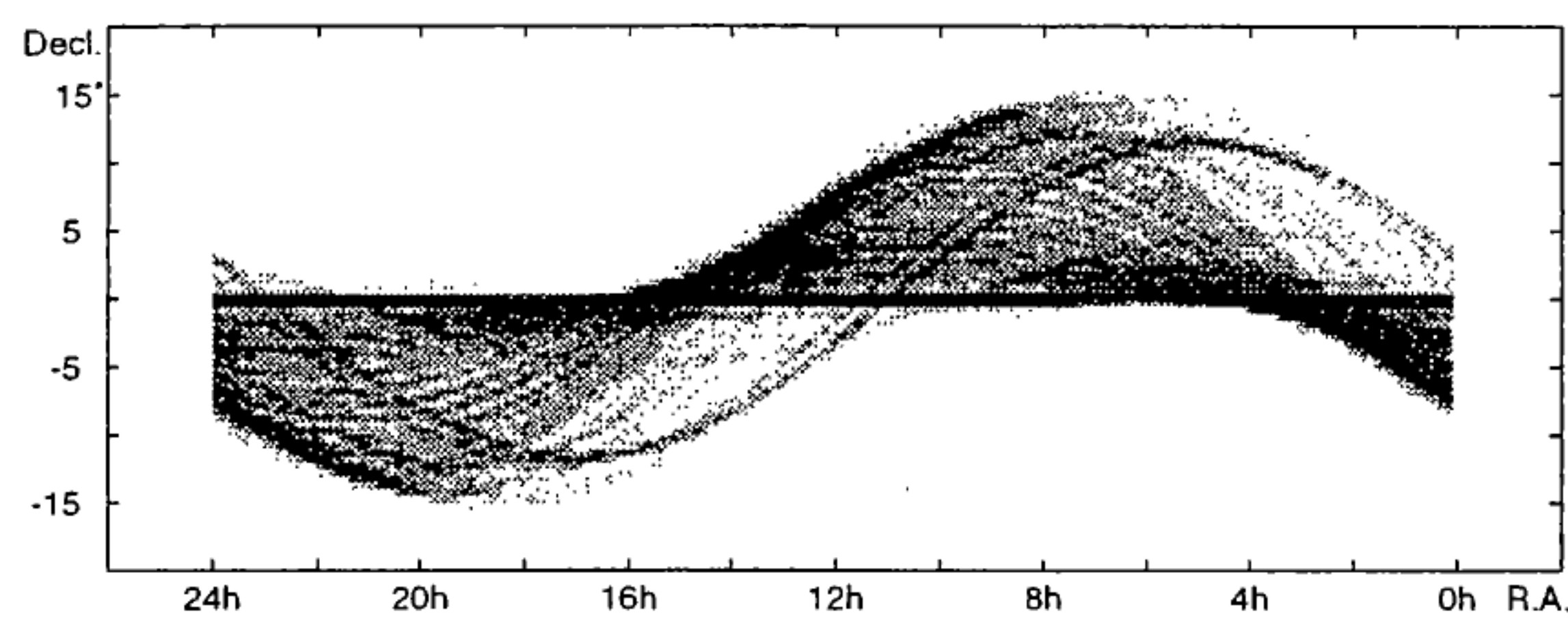


Figure 4. Density of catalogued GEO objects on the celestial sphere in a logarithmic scale, black corresponds to the highest density (geocentric view, elements from Ref. 5).

The mean object density is maximum along the geostationary ring with values between 0.4 and 0.8 objects/deg<sup>2</sup>. The highest density is recorded at right ascensions 4.3h and 16.3h where the orbits with inclination between  $3^\circ$  and  $7^\circ$  cross the equator. At the 'caustic' the object density is still of the order of 0.5 objects/deg<sup>2</sup>. For test purposes or for specific surveys the detection probability may therefore be increased by observing at the locations with increased object density. It may be assumed that the majority of the uncatalogued objects follow similar orbits as the catalogued ones. However, populations may exist with orbital characteristics significantly differing from those of the catalogued population.

#### 4.2. Expected Detection Rates

From the Zimmerwald observatory (longitude  $7.5^\circ$  E, latitude  $46.9^\circ$  N) a sector of  $93^\circ$  is observable above  $20^\circ$  elevation (from  $54^\circ$  E to  $39^\circ$  W). With the field of view of  $0.2 \text{ deg}^2$  used for the survey presented below and assuming a maximum of 1260 frames per

night (7 hours of observations, 20 seconds per frame) and double exposure of each field, 22 nights would be required to cover a band of  $\pm 15^\circ$  along the geostationary ring visible from Zimmerwald (i.e.  $2760 \text{ deg}^2$ ). On the average an uncatalogued object will be found on every hundredth field. To cover a stripe with a width of  $1^\circ$  along the geostationary ring,  $470 \times 2$  exposures are required. Such a program may be carried out in one single night.

It is, of course, very difficult to estimate the expected detection rates for uncatalogued objects. For a rough estimate we refer to the findings of Talent et al. (Ref. 6) in the context of a NASA survey of space objects near the geostationary ring. This study reports a mean object density of 0.046 objects/deg<sup>2</sup> for objects brighter than 17-th magnitude. About 25% of the objects observed were uncatalogued. Adapting these numbers to the Zimmerwald telescope we expect one uncatalogued object brighter than 17-th magnitude in 95 fields. Using the size distribution for objects in LEO — due to lack of information — for extrapolating the detection rates to fainter magnitudes gives one uncatalogued object brighter than magnitude 18.5 in 60 fields (see Table 1).

magnitude	17.0	17.5	18.0	18.5	19.0
object size (m)	0.58	0.46	0.37	0.29	0.23
fields/obj	95	87	70	60	50

Table 1. Expected detection rates for uncatalogued objects (based on extrapolation of the results of Talent et al. (Ref. 5) and assuming a geometrical albedo of 0.08) for a field of view of  $0.2 \text{ deg}^2$ .

### 5. SHORT OBSERVATION CAMPAIGN

#### 5.1. Set-up of the Test Campaign

A very limited survey near the geostationary ring was carried out during seven nights in February and March 1997 with the Zimmerwald telescope. Because the  $2k \times 2k$  pixel CCD camera was not ready the  $512 \times 512$  pixel CCD camera used instead in the F/1.2 focus which is normally used for the TV camera for visual tracking of Laser satellites. However, the F/1.2 focal reducer optics has relatively strong vignetting and coma. In addition, the CCD camera had to be used without shutter due to the very short backfocus distance. The image scale was  $3.4''$  per pixel. Nevertheless the relatively poor optical quality of the frames (point sources are spread over several pixel) allowed to take  $2 \times 2$  binned frames. The limiting magnitude for a 5 second exposure was about  $16 m_v$  in the center of the field and one magnitude less at the borders of the frames (estimated using photometric standard stars). This result seems to



be surprising for a 1 m telescope. It is, however, due to the bright sky background of  $19 \text{ m}_v$  per square arcsecond in Zimmerwald and the large effective image scale of  $6.4''$  per pixel. In fact the sky background per pixel is of the order of  $15 \text{ m}_v$ ! This is the main reason to use the F/4 focus for future surveys.

During each of the seven nights a number of series were acquired, all containing 40 frames. The individual frames were exposed for 5 seconds and spaced by 40 seconds. All exposures were made with fixed telescope in order to maximize the S/N for geostationary objects. Between exposures the sidereal motion was compensated to allow the use of the same reference frame for the entire series. The computer control of telescope and camera allowed automatic execution of this stop-and-resume procedure. The separation of the individual frames gave an overlapping factor for one field (in earth-fixed frame) of about 2.7.

The first frame in each series was flat-field reduced and then used for the generation of a mask of the brightest stars. The strong vignetting made it necessary to take the difference of each search frame and the reference frame prior to the application of the mask. Masking was still required because bright stars do not completely disappear on the difference frame due to photon noise and seeing. The masked difference frame was finally scanned automatically for moving objects. In order to control the performance of the automatic procedures the operator inspected the search frames visually at the screen. Eventually a circular orbit was determined for each observed object. The orbits were available in near real-time, i.e., about 15 minutes after the acquisition of the frames. Except for the controlled objects no attempt was made to identify the observed objects because the current version of the catalogue was not available in electronic form at the observatory.

The fields were selected close to the Earth's shadow in order to maximize the phase angle. The Milky Way was avoided to reduce the stellar background. Finally regions with increased density of catalogued objects at the sky were selected. Fields along the equator (the parallax of the geostationary ring is about  $-7^\circ$  for Zimmerwald) close to the descending nodes of orbits with inclination of  $7^\circ$  as well as fields along the 'caustic' in Figure 4 for given orbital inclinations were selected. Thereby we tried to maximize the detection rate. The fields used for the small survey are listed in Table 2.

## 5.2. Results

Between February 21 and March 13, 1997, 1961 exposures covering different regions near the geostationary ring were acquired at the Zimmerwald observatory. With the field of view of  $0.2 \text{ deg}^2$  and a covering factor of about 2.7 this corresponds to a survey area of  $152 \text{ deg}^2$ . The total observation time was 21.8 hours.

The distribution of the search fields in the Earth-fixed frame is given in Figure 5 together with the locations of the observed objects. In the geostationary ring all controlled objects that were reported to be in the search fields, were successfully observed. In addition to these 33 objects a total of 25 objects with inclinations exceeding  $0.5^\circ$  were found. It may be assumed that most of them are uncontrolled objects although some controlled satellites have inclinations of more than  $5^\circ$ . Depending on the location of the observation fields in the sky the expected number of objects with inclinations exceeding  $0.5^\circ$  was computed using the density distribution of Figure 4. The expected and the observed number of objects for our fields are given in Table 2. The observed number of objects is in agreement with the number expected from the catalogue. The small number of objects is, however, also in accordance with 25% of uncatalogued objects claimed in Ref. 6. In Figure 6 the distribution of the inclination v.s. the right ascension of the ascending node is given for the orbits of the observed objects (circular orbit assumed) and the catalogued objects from Ref. 5.

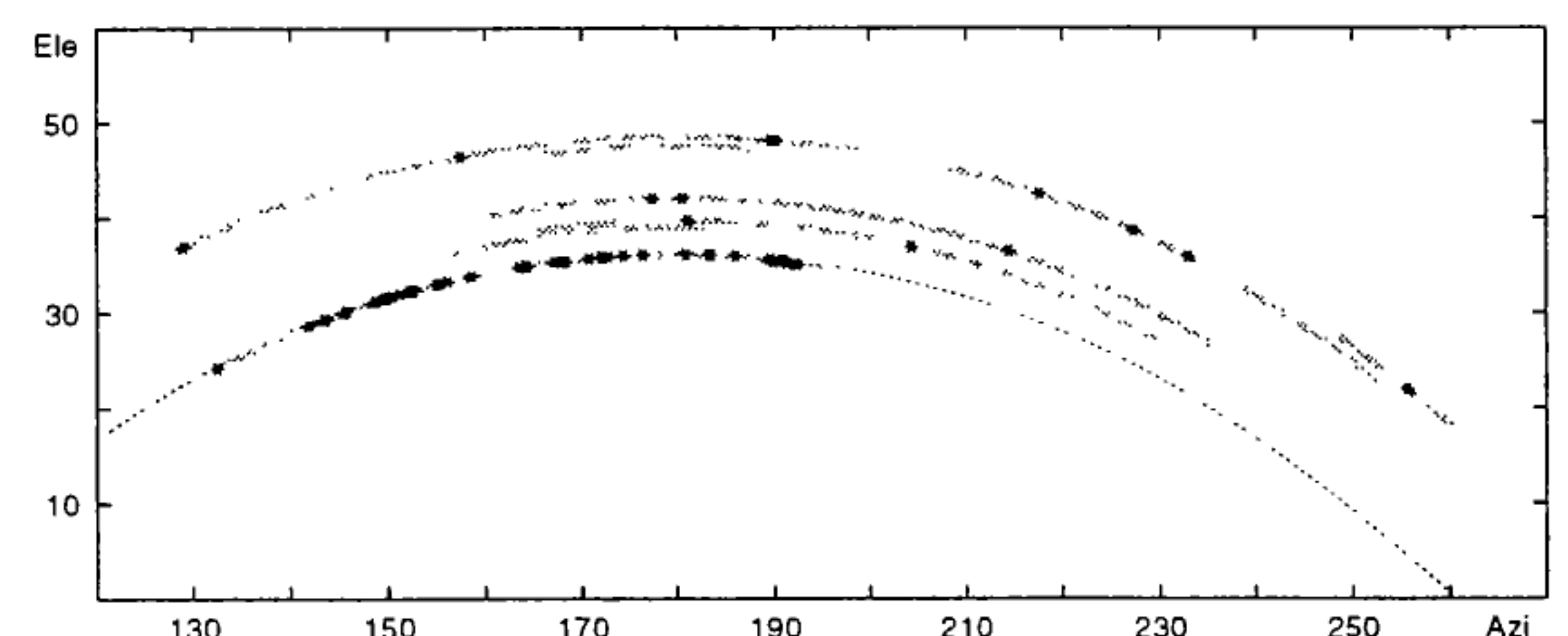


Figure 5. Distribution of the search fields of the limited survey carried out at Zimmerwald (shaded areas). The symbols (\*) indicate observed GEO objects, the dashed line represents the location of the geostationary ring.

## 6. CONCLUSIONS

Ground based optical observations may significantly enhance the knowledge on the space debris environment in particular in the GEO and GTO region where Radar observations are limited to objects larger than 1 meter. To perform efficient surveys large fields of view are required, and on-line data pro-



Date	Position		Orbit Characteristics	Number of Frames	Area [deg <sup>2</sup> ]	Objects	
	R.A.	Decl.				expected	observed
21/22 Feb. 97	13h00m	-7°00'	node $i = 14^\circ$	80	6.1	0.2	0
	16h15m	-7°00'	node $i = 7^\circ$	160	12.1	5.1	4
22/23 Feb. 97	16h17m	-7°00'	node $i = 7^\circ$	205	18.2	5.4	4
6/7 Mar. 97	8h30m	+6°40'	culm. $i = 12^\circ$	80	6.1	0.1	1
	14h30m	-7°40'	node $i = 12^\circ$	120	9.1	0.7	3
	15h00m	-7°20'	node $i = 12^\circ$	40	3.0	0.6	1
8/9 Mar. 97	10h03m	+5°24'	caustic $i = 13^\circ$	493	37.5	6.3	7
9/10 Mar. 97	14h19m	-3°24'	caustic $i = 7^\circ$	160	18.3	0.4	2
11/12 Mar. 97	13h07m	+4°24'		80	6.1	0.0	0
	14h52m	-4°12'	caustic $i = 6^\circ$	106	8.1	0.2	0
12/13 Mar. 97	13h07m	-1°06'	caustic $i = 9^\circ$	357	27.2	2.3	3
Total:				1961	152	21.2	25

Table 2. Distribution of observations, position of search frames on the celestial sphere and characteristics of orbits of uncontrolled objects crossing the field, number of frames and area covered, number of expected catalogued objects with inclination  $i > 0.5^\circ$  and observed number.

cessing capabilities are mandatory to cope with the data flows.

A circular orbit determined from two closely spaced observations of a detected object gives an orbital inclination and right ascension of the ascending node which are reliable enough for tracking the object within the following hour(s) and for reducing the number of possible candidate objects for identification.

The uneven density distribution (Figure 4) of geostationary objects in the celestial sphere allows to select regions of increased density for a particular search scenario (at least for tests of the performance).

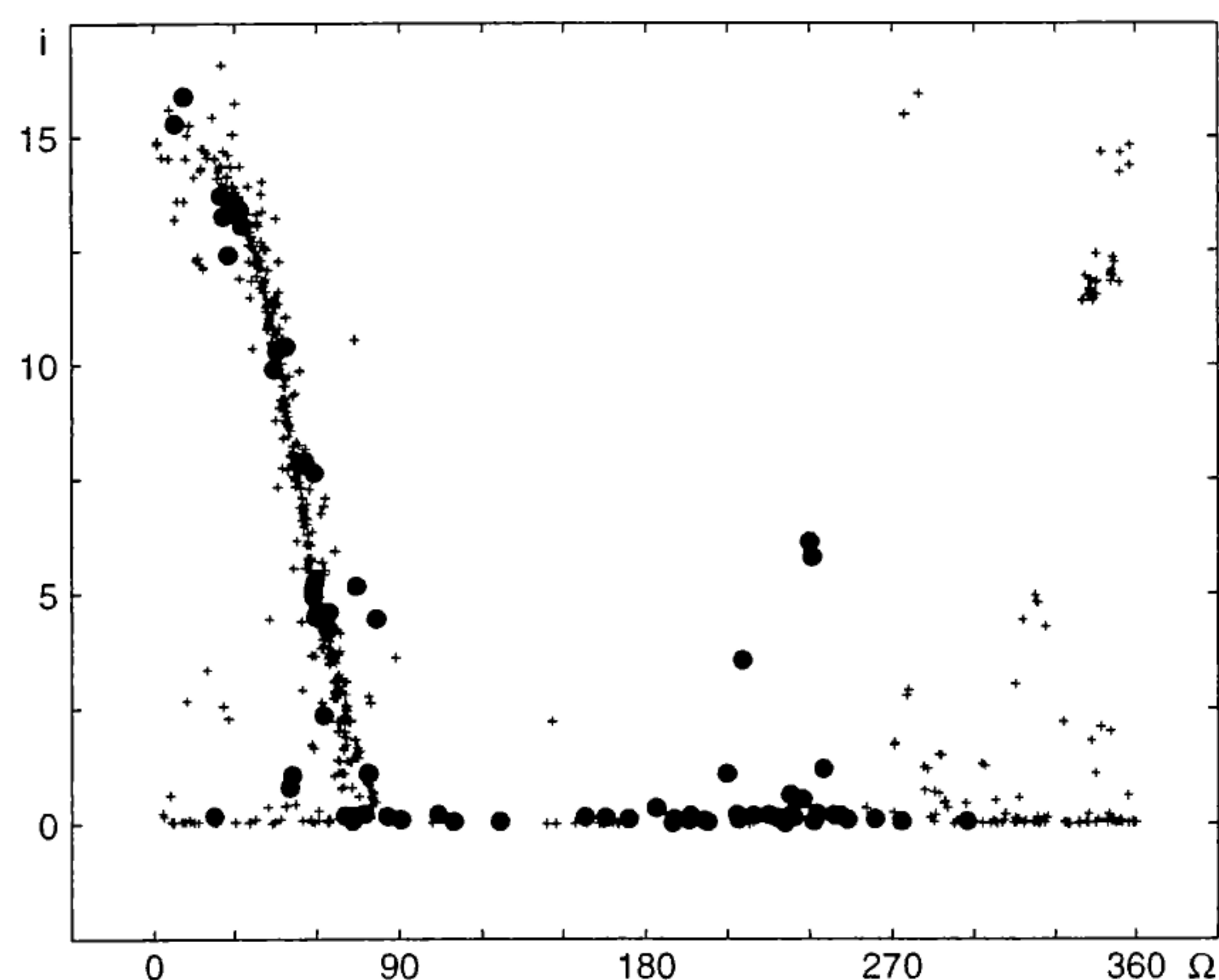


Figure 6. Distribution of inclination v.s. right ascension of the ascending node for the observed objects (•) and the catalogued objects (+).

A very limited GEO survey (1961 exposures, 152 deg<sup>2</sup>) was performed using the Zimmerwald 1 meter telescope. The number of observed uncontrolled objects is in agreement with the expected number of catalogued objects. Given the small number of observed objects the result is also consistent with a possible 25% incompleteness of the catalogues as reported in other studies (Ref. 6).

## 7. REFERENCES

1. Schildknecht, T., Hugentobler, U., and Verdun, A., CCD Algorithms for Space Debris Detection, *ESA Study Final Report*, ESA/ESOC Contract No. 10623/93/D/IM, 1995
2. *Interagency Report on Orbital Debris*, Office of Science and Technology Policy, The National Science and Technology Council, 1995.
3. Henize, K. G., Stanley, J., Optical Observations of Space Debris, *Orbital Debris: Technical Issues and Future Directions*, A. E. Potter (Ed.), NASA Conference Publication 10077, pp. 241-244, 1992.
4. Allan, R. R., Cook, G. E., The Long-Period Motion of the Plane of a Distant Circular Orbit, *Proc. Roy. Soc. London*, 280A, pp. 97-109, 1964.
5. Janin, G., *Log of Objects near the Geostationary Ring*, Issue 16, ESOC, February 1996.
6. Talent, D. L., Potter, A. E., and Henize, K. G., A Search for Debris in GEO, in *Proceedings of the Second European Conference on Space Debris*, W. Flury, (Ed.), Darmstadt, Germany, March 17-19, 1997.